Paper presented at International Conference on
Electrical Engineering (ICEE) 2015, HongKong, China, 5-9 July, 2015

Comparison and Analysis of Methods to Prevent DC Power Discontinuation of Hybrid HVDC

XIAOBO YANG[1], BERNT BERGDAHL[2], CHUNMING YUAN[1], DAWEI YAO[1], CHAO YANG[1]

1. Corporate Research, ABB (China) Limited 2. ABB AB, Sweden
xiaobo.yang@cn.abb.com

Abstract

Hybrid HVDC with line commutated converter (LCC) as rectifier and voltage source converter (VSC) as inverter has prospective applications for the long distance DC power transmission, the power-from-shore power system and the city in-feed etc. One technical challenge of hybrid HVDC is to avoid or mitigate the DC power discontinuation during AC voltage decreases at the LCC rectifier side. The DC power discontinuation will give a disturbance in the receiving end AC system. To solve this issue, the paper proposed a new solution, which is to increase the nominal firing angle of LCC during nominal operation to maintain the DC voltage control during LCC AC voltage decrease. Compared with other solutions e.g. the full bridge and half bridge sub modules based MMC (FHMMC), the proposed solution has smaller valve losses and less modifications on existing HVDC control system. In this paper, a typical hybrid HVDC model is established firstly; the required nominal firing angle and main parameters of LCC are determined considering the transient DC voltage decrease caused by the line fault at the AC system of LCC rectifier side; finally, additional power losses and reactive power assumption of the propose solution are calculated and compared to FHMMC design.

Keywords
HVDC, Hybrid HVDC, LCC, MMC

1. INTRODUCTION

The line commutated converter (LCC) HVDC so far is the major HVDC solution with advantages of large capacity and lower cost, while it has large footprint and high reactive power requirement. On the other hand, the voltage source converter (VSC) HVDC employs self-commutated converter, which consists of gate turn-off components thus brings compact size and decoupled active/reactive power control flexibility. However, nowadays the VSC HVDC still has higher cost and power losses than those of the LCC-HVDC. To leverage the advantages of both VSC HVDC and LCC HVDC, a hybrid type HVDC system, which has one VSC terminal and one LCC terminal in the same HVDC system, was proposed and studied in past years[1][2][3][4][5][6] [7][8]. The hybrid HVDC system can be categorized into two basic types, namely LCC-VSC type and VSC-LCC type, as shown in Fig. 1.

LCC-VSC type hybrid HVDC system has extensive application prospects for the long distance DC power transmission, the power- from-shore power system and the city in-feed [1][2][3][4][5][6].

VSC-LCC type hybrid HVDC system has potential application for offshore wind farm connection, whereas the LCC inverter will risk commutation failure and the system is difficult to realize black start for offshore wind farm[7][8].

In this paper, only the LCC-VSC hybrid HVDC system will be discussed and be abbreviated as hybrid HVDC hereafter.

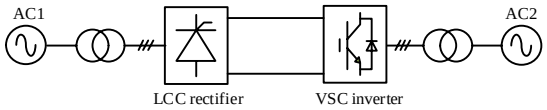

(a) LCC-VSC type: LCC as rectifier, VSC as inverter

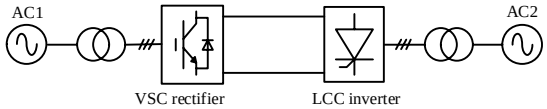

(b) VSC-LCC type: VSC as rectifier, LCC as inverter

Fig. 1 Configurations of hybrid HVDC systems

Although the hybrid HVDC synergizes the advantages of both LCC and VSC, it suffers from the special issues caused by the hybrid combination. One technical issue observed is the DC power discontinuation during AC voltage decrease at the LCC rectifier. Normally, when the AC voltage of the LCC rectifier drops, the firing angle of LCC (α) will decrease accordingly to keep the DC current or DC voltage following the respective current or voltage order. However, if the amplitude of the AC voltage decreases further (larger than 3%), α reaches its minimum value α_{min} hence the LCC rectifier will lose its DC current controllability during this transient process. After that, the DC current begin to decreases. Because the control margin of modulation index (m) at VSC inverter is usually small, it will increase to its upper limit m_{max} quickly

and also lose its power controllability. Finally the DC current decreases to zero which results in a discontinuous DC power transmission until the AC fault is recovered to normal range.

The DC power discontinuation will give a disturbance at the receiving end AC system. To solve this issue, there are two different technical roadmaps: one is to use full bridge submodule (FBSM) based modular multilevel converter (MMC) topology for VSC, the other is to reconfigure the steady state operation points of the system to obtain larger DC voltage controllability.

A) FBSM based MMC

Because the FBSM can change its voltage among positive, negative and zero in its output port, a large DC voltage variation in FBSM based MMC (FBMMC) is allowable by using proper control and modulation method [9]. However, the total IGBT number of FBMMC is twice of the half bridge sub module based MMC (HBMMC) which results in remarkable high power losses and high cost. One trade-off is to employ both half bridge submodules (HBSMs) and full bridge submodules (FBSMs) in each arm of MMC [10], namely FHMMC. The number of FBSMs in the FHMMC is designed based on the pre-defined minimum DC voltage during LCC AC voltage decrease. By this way both IGBT number and power losses are decreased to some extent. However, the power losses of the hybrid MMC is still higher than that of half bridge based MMC while the modulation algorithm becomes complex.

B) Reconfiguration of steady state operation points

By changing the steady state operation points of the LCC or VSC in the hybrid HVDC system, larger control margin of DC voltage can be obtained. In theory, either high nominal firing angle (α_N) of LCC or low nominal modulation index (m_N) of VSC can realize larger control margin during AC voltage decrease at LCC. However, lower m_N will cause much higher power losses in the VSC IGBT valves due to high RMS value of valve current during nominal operation thus not recommended. On the contrary, if the nominal α_N of LCC is designed appropriately, the additional power losses at LCC valve and converter transformer are relatively smaller than the FHMMC solution.

In this paper, the reconfiguration of steady state operation points of LCC is proposed. The paper is organized as follows. In Section 2, a hybrid HVDC model is established; the main parameters and the control strategy of the hybrid HVDC are introduced; the basic control strategy is presented; the cause of the DC power discontinuation is analyzed. In Section 3, the design criteria of LCC for system steady state operation is presented. The required nominal α_N of LCC is calculated. In Section 4, the additional power losses caused by the proposed method are calculated and compared with conventional design and the FHMMC solution.

2. ANALYSIS

2.1 Model description

A ±400kV/800MW hybrid HVDC bipolar model is established and used for the analysis in this paper. The system consists of an LCC as rectifier station, a VSC as inverter station and 300 km long ±400kV transmission lines connecting between the stations. The LCC station has a configuration with a 12-pulse thyristor valve group. The VSC station uses the MMC topology at each pole. The short circuit ratios (SCRs) at 500kV AC bus voltages of both LCC rectifier station and VSC inverter station are set to 5. The system is grounded directly at both converter stations.

Each pole of the system has a diode valve (D_l) placed at the DC line side of VSC inverter to block the DC fault current contributed from VSC during DC line faults[11][12][13].

The single line diagram of the hybrid HVDC is shown in Fig. 2.

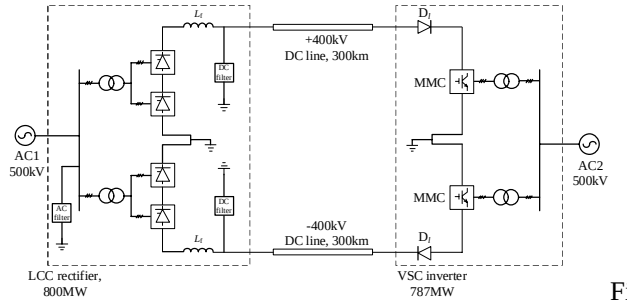

Fig. 2 The simplified diagram of the hybrid HVDC

The main parameters of the hybrid HVDC model is listed in Table 1, in which the nominal DC voltage of LCC and VSC, U_{dNR} and U_{dNI}, are defined as the voltages cross the DC line and ground respectively.

Table 1 Main parameters of the hybrid HVDC model

Quantity	Value	Description
P_{dN}	800 MW	Nominal DC power (bipole)
R_d	7.3 Ω	DC Line resistance
I_{dN}	1 kA	Nominal DC current
Parameters of LCC		
U_{lNR}	530 kV	Nominal AC voltage of LCC
U_{dNR}	400 kV	LCC Nominal DC voltage
U_{dNI}	385.5 kV	VSC nominal DC voltage
α_{min}	5°	Min. firing angle

d_{xR}	9%	Relative inductive voltage drop
d_{rR}	0.3%	Relative resistive voltage drop
U_T	0.15 kV	LCC valve forward voltage drop
Parameters of VSC		
m_{max}	0.88	Maximum modulation index
N	23	Number of SMs per arm

In this paper, the modulation index of VSC m is defined as the ratio between the fundamental AC output voltage U_m (phase to ground, peak value) and $4/\pi\cdot(U_{dI}/2)$, where U_{dI} is the direct voltage of DC line to ground, as showed in (2-1):

$$m = \frac{\pi}{4}\frac{U_m}{U_{dI}/2} \tag{2-1}$$

2.2 Basic control strategy

There are two basic control modes for hybrid HVDC according to which station is in charge of DC voltage control or DC current control:

Mode 1: the LCC rectifier controls the DC voltage while the VSC inverter controls the DC current;

Mode 2: the LCC rectifier controls the DC current while the VSC inverter controls the DC voltage.

The nominal steady state U_d-I_d characteristics of the two control modes at are illustrated in Fig. 3**Error! Reference source not found.** (a) and (b) respectively, in which I_{dN} is the nominal DC current, U_{dNR} is the nominal DC voltage of LCC, U_{dNI} is the nominal DC voltage of VSC. $U_{dabsminI}$ is the absolute minimum DC voltage at VSC side. For the harmonic injected PWM (HIPWM) strategy, $U_{dabsminI}= m_{absmax}\cdot U_{vNI\_pk}$, where U_{vNI_pk} is the peak value of the nominal phase-phase AC voltage at valve side of VSC phase reactor.

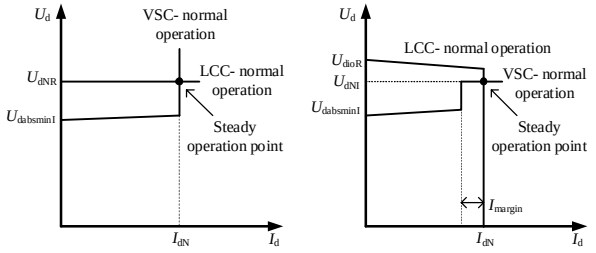

(a) control mode 1 (b) control mode 2

Fig. 3 Simplified U_d-I_d characteristics

Both of the two modes can be used for control of hybrid HVDC. However, for control mode 2, the current margin control, which has been widely employed at classical HVDC system, it is still necessary with complex control system [16] and tele-communication between LCC and VSC.

The control mode 1 is used for the analysis in in this paper. If not otherwise specified, the control strategy of hybrid HVDC hereafter refers to the control mode 1. It should be noted that the analysis method below is also applicable for control mode 2, though it is not discussed due to the limitation of the paper length.

The simplified control diagram for hybrid HVDC is shown in Fig. 4. The DC voltage of LCC is controlled directly by the PI controller. The DC current control of VSC is controlled indirectly by the active power control loop inside the DC power controller of VSC.

During nominal operation, a steady operation point (as shown in Fig. 3**Error! Reference source not found.** (a)) is established automatically.

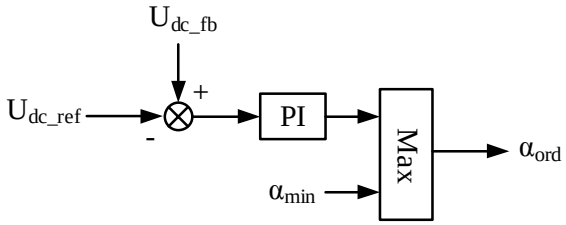

(a) DC voltage controller of LCC

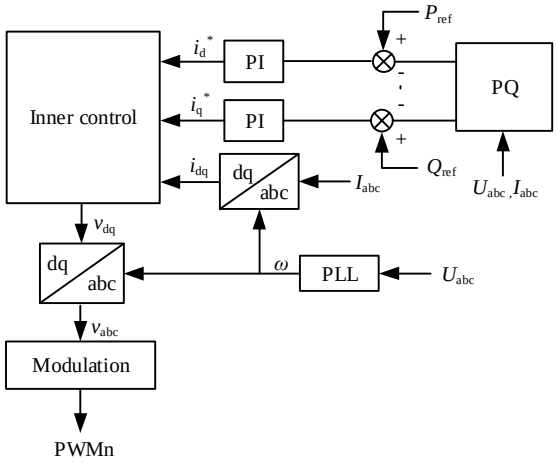

(b) DC power controller of VSC

Fig. 4 Simplified control diagram of Hybrid HVDC

2.3 DC power discontinuation during AC voltage of LCC

The control characteristics of hybrid HVDC during LCC AC voltage decrease is shown in Fig. 5 and explained as below. When AC voltage at LCC side has small decrease, LCC will reduce its firing angle α to a lower value to keep the DC voltage follow its DC voltage order. After α reaches the minimum firing angle limit α_{min}, the U_d-I_d curve of LCC will degenerate to an oblique line (figured in dash line). At the same time, VSC keeps its constant DC current control. The operation point is shifted from point A to point B. The operation point transition is finished automatically under the independent control of LCC and VSC and the telecommunication is not needed. However, when the AC voltage of LCC keeps on decreasing, the DC line voltage will drop further and cannot overcome the DC voltage at VSC from anti-parallel diodes (the U_{di0I}). Finally the VSC controller loses its DC power controllability and consequently the DC power decreases to zero.

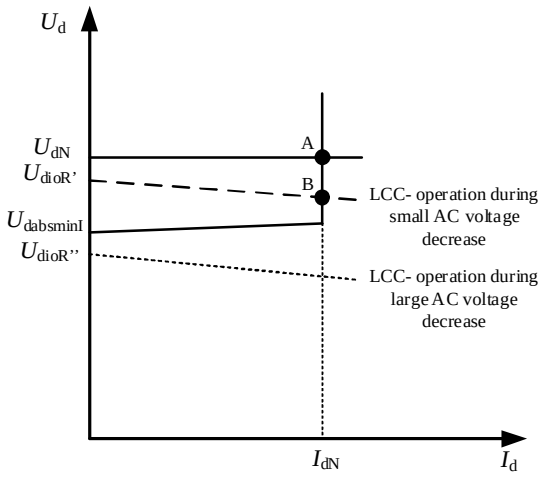

Fig. 5 U_d-I_d characteristics of hybrid HVDC

It can be seen from Fig. 5 that the boundary condition of the DC power continuation is $U_{di0R} \leq U_{absminI}$. To increase the control margin of the hybrid HVDC, a straight forward method is to increase the value of U_{di0NR}, i.e. increase the nominal firing angle. This method is straight forward and doesn't impact the conventional control strategy for hybrid HVDC. However, the proposed method cannot prevent the DC power discontinuation during severe AC fault at LCC, for example the 3-phase to ground AC fault happens near AC bus. However, such a serious AC fault means that the HVDC system can hardly transmit power and it is not necessary to design the hybrid MTDC system to ride through this critical case. According to [17], an AC fault on the lines connected to the AC bus of the LCC will mainly result in 10% to 20% decreasing of AC bus voltage. In this paper, the minimum AC voltage for guaranteed active power can be defined as 80~90% of the nominal AC voltage of LCC, and denoted as U_{acmin}.

3. MAIN PARAMETERS DESIGN

3.1 Main parameters of LCC

A) Calculation of nominal firing angle

The DC voltage of LCC is calculated according to the following equation:

$$\frac{U_{\mathrm{dR}}}{n}=U_{\mathrm{di0R}}\left(\cos\alpha-(d_{\mathrm{xR}}+d_{\mathrm{rR}})\frac{I_{\mathrm{d}}}{I_{\mathrm{dN}}}\frac{U_{\mathrm{dioNR}}}{U_{\mathrm{dioR}}}\right)-U_{\mathrm{T}} \tag{3-1}$$

Where n is the number of 6-pulse bridges.

For nominal operation with nominal AC voltage and nominal DC power, the no-load direct voltage of LCC U_{di0NR} can be calculated as:

$$U_{\mathrm{di0NR}}=\frac{\frac{U_{\mathrm{dNR}}}{n}+U_T}{\cos\alpha_{\mathrm{N}}-\left(d_{\mathrm{xR}}+d_{\mathrm{rR}}\right)} \tag{3-2}$$

During the LCC AC voltage suppression to U_{acmin}, firing angle of LCC decreases to α_{min} while the nominal DC voltage and DC current are still guaranteed. Thus the ideal no-load direct voltage during AC voltage decrease is expressed as:

$$U'_{\mathrm{di0R}}=\frac{\frac{U_{\mathrm{dNR}}}{n}+U_T+\left(d_{\mathrm{xR}}+d_{\mathrm{rR}}\right)\cdot U_{\mathrm{di0NR}}}{\cos\alpha_{\mathrm{min}}} \tag{3-3}$$

Since U_{di0R} is proportional to the AC voltage, it gives:

$$U'_{\mathrm{di0R}}=\frac{U_{\mathrm{acmin}}}{U_{\mathit{l}\mathrm{NR}}}\cdot U_{\mathrm{di0NR}} \tag{3-4}$$

The no-load direct voltage and firing angle during nominal operation can be solved by combination of (3-1), (3-2) and (3-3) and (3-4).

B) Calculation of reactive power consumption

For high firing angle operation, the reactive power consumption of LCC will increase and need to be investigated.

The reactive power consumption per pole is calculated as:

$$Q_{\mathrm{dR}}=2\cdot\chi\cdot I_{\mathrm{d}}\cdot U_{\mathrm{di0R}} \tag{3-5}$$

where χ is the function of firing angle α and overlap angle μ, defined as:

$$\chi=\frac{1}{4}\cdot\frac{2\cdot\mu+\sin 2\alpha-\sin 2\left(\alpha+\mu\right)}{\cos\alpha-\cos\left(\alpha+\mu\right)} \tag{3-6}$$

4. POWER LOSSES

In this section, the power losses of the proposed solution are calculated. Besides, the power losses of LCC with conventional firing angle design (α_{NR}=15°) and the power losses of VSC with FHMMC solution are also calculated for comparison.

4.1 Power losses of proposed solution

By far there is no standard calculation procedure for power losses of LCC due to its complexity and project dependent. However, it is known that the losses from thyristors and the converter transformers contribute 71-88% of the total power losses of the converter station [18]. In this section, the thyristor conductive losses and converter transformer losses is calculated, based on the calculation procedure in [18].

A) Calculation prerequisites

The parameters used for power losses calculation are listed in Table 2.

Table 2 The parameters for power losses calculation

Quantity	**Description**	**Value**
Thyristor parameters		
V_{T0}	Thyristor conducting voltage drop	1.25V
R_0	Thyristor conducting resistance	0.48 mΩ
n_1	number of thyristors per valve	60
n_2	number of single valves per pole	12
LCC converter transformers		
$P_{(\mathrm{loss1})}$	Power losses of transformer at rated frequency current	600kW

B) Power loss of thyristor valves

Only the conductive power loss is calculated, which is the main part of the valve losses. The valve conductive power loss P_1 is calculated as:

$$P_1=\frac{n_1 I_d}{3}[U_{T0}+R_0 I_d(\frac{2\pi-\mu}{2\pi})] \tag{3-7}$$

Where I_{d} is the DC current flows through the valve.

The total conductive power losses of one pole is calculated as:

$$P_v=n_2 P_1 \tag{3-8}$$

C) Power loss of converter transformer

The 3-phase, 3 windings converter transformer loss is calculated as:

$$P_{\mathrm{tr}} = 3 \cdot \sum_{\mathrm{n}=1}^{49} I_{(\mathrm{h})}^2 R_{(\mathrm{h})} \qquad (3\text{-}9)$$

Where I_{h} is the RMS value of the h[th] harmonic current; $R_{(\mathrm{h})}$ is the effective resistance for the h[th] harmonic current. As a rough estimation, the total power transformer losses only include the rated frequency current loss and 11[th], 13[th], 23[rd] and 25[th] harmonic current losses.

4.2 Power losses of conventional LCC solution

The power losses calculation procedure for LCC with conventional firing angle design is the same as that for high firing angle solution.

For α_{NR}=15°, U_{di0NR} is 249.1 kV.

The power losses calculation results for conventional firing angle design will be presented in Sections 5.

4.3 Power losses of an alternative FHMMC solution

A) Required number of full bridge sub modules

In this analysis it is assumed that in the FHMMC solution is based on N half bridge SMs (Table 1) and in addition M full bridge SMs. Reference [10] gives the calculation criterion of the required minimum number of FBSM in the FHMMC with given minimum DC voltage, which can be modified as:

$$-M_{\eta} \cdot U_{\mathrm{c}} \le \frac{1}{2} U_{\mathrm{dNI}} \left(\eta - \frac{m_{\max}}{m_{\mathrm{absmax}}}\right) \qquad (3\text{-}10)$$

Where M_{η} is the number of the FBSM in each arm of FHMMC; η denotes the minimum DC voltage in p.u. value during AC voltage decrease. U_{c} is the nominal DC voltage of sub module. In this analysis the same U_{c} is assumed for the full bridge SMs as for the half bridge SMs, U_{c}=17.1 kV in this paper. $m_{\max}$ is the maximum modulation index for steady state operation including control margin. m_{absmax} is the absolute maximum modulation index. With the definition of (2-1), m_{absmax} is calculated as:

$$m_{\mathrm{absmax}} = \frac{\pi}{4} \frac{\mathrm{U}_{\mathrm{dI}} / \sqrt{3}}{U_{\mathrm{dI}} / 2} \qquad (3\text{-}11)$$

which gives

$$m_{\mathrm{absmax}} = \frac{\pi}{2\sqrt{3}} = 0.907$$

The total number of SMs at each arm can be calculated as:

$$N_{\eta} + M_{\eta} = \frac{U_{\mathrm{dNI}}}{U_{\mathrm{c}}} \qquad (3\text{-}12)$$

Where N_{η} is the number of the HBSM in each arm.

It can be calculated from (3-10) and (3-11) that for nominal operation (i.e. η=1), $M_{1.0}$=0 and $N_{1.0}$=23.

During the LCC AC voltage suppression, the nominal DC power at VSC side should be guaranteed, and η can be calculated based on the following set of equations:

$$U_{\mathrm{dI}}^{'} = \eta \cdot U_{\mathrm{dNI}} \qquad (3\text{-}13)$$

$$U_{\mathrm{dNI}} \cdot I_{\mathrm{dN}} = U_{\mathrm{dI}}^{'} \cdot I_{\mathrm{d}}^{'} \qquad (3\text{-}14)$$

$$U_{\mathrm{dI}}^{'} = U_{\mathrm{dR}}^{'} - R_{\mathrm{d}} \cdot I_{\mathrm{d}}^{'} \qquad (3\text{-}15)$$

$$\frac{U_{\mathrm{dR}}^{'}}{n} = U_{\mathrm{di0R}}^{'} \left(\cos\alpha_{\min} - (d_{\mathrm{xR}} + d_{\mathrm{rR}}) \frac{I_{\mathrm{d}}^{'}}{I_{\mathrm{dN}}} \frac{\mathrm{U}_{\mathrm{di0NR}}}{U_{\mathrm{di0R}}^{'}} \right) - U_{\mathrm{T}} \qquad (3\text{-}16)$$

Where U_{di0NR} is the no-load DC voltage of LCC (with α_{NR}=15°), U'_{dR}, U'_{di0R}, U'_{dI} and I'_{d} are the DC voltage of LCC, the no-load DC voltage of LCC, DC voltage of VSC and DC current during the LCC AC voltage decrease respectively.

B) Power losses evaluation

The additional losses come from the full bridge SMs. assume that the power loss of a FBSM are as twice as that of a HBSM, the total increased power losses of Hybrid MMC valve can be calculated as:

$$\Delta P = \left(1 + \frac{M_{\eta}}{M_{\eta} + N_{\eta}}\right) \times 100\% \qquad (3\text{-}17)$$

Where M is the number of FBSM and N is the number of HBSM in each arm of MMC.

5. COMPARISON AND ANALYSIS

A) Comparison with conventional design of hybrid HVDC

For decreased AC voltage operation, the main parameters and power losses of the high firing angle solution and FHMMC solution are listed in
Table 3. The main parameter and losses of conventional design (with α_{NR}=15° for LCC, HBMMC for VSC) are also listed for benchmark. The additional power losses are presented in p.u. value. The calculation cases in
Table 3 are defined as below:
Case 1: Benchmark case with conventional design, i.e. α_{NR}=15° and HBMMC topology for VSC inverter;
Case 2: Design to guarantee normal power transmission during U_{acmin}=90% U_{lNR};
Case 3: Design to guarantee normal power transmission during U_{acmin}=85% U_{lNR}.

B) Analysis

It can be concluded from
Table 3 that the additional valve conductive losses for high firing angle design is rather small and can be neglected. The additional power losses from converter transformers are also small. However, high firing angle operation results in higher U_{di0NR} and larger reactive power consumption, thus both thyristor number and AC filter capacity are increased. For case 2, i.e. U_{acmin}=90%·U_{lNR}, the total valve power losses are increased to 108.6% and the reactive power assumption is increased to 135%, compared with conventional design. If the AC voltage decreases further (Case 3), the nominal firing angle will increase greatly and results in much larger reactive power consumption. Thus the high firing angle design solution is applicable for U_{vRmin}>90%·U_{lNR}.

For FHMMC solution, the additional full bridge SMs brings additional power losses. In Case 2 and Case 3, the power losses are increased to 104% and 109% respectively. The total power losses of VSC valve in FHMMC solution is slightly smaller than the total power losses of LCC in high firing angle solution. Besides, the power losses of VSC converter transformer in FHMMC solution is not changed because the VSC AC side operation condition is the same as for Case 1 (the benchmark). Therefore, if the operation during large LCC AC voltage decease is required (U_{vRmin}<90%·U_{lNR}), the FHMMC solution is preferred due to its less power losses and less primary equipment dimensioning.

Table 3 Comparison of the proposed solution the FHMMC solution and conventional design

	Case 1 Benchmark	**Case 2 90% of U_{lNR}**	**Case 3 85% of U_{lNR}**
High firing angle solution			
Nominal firing angle, α_{NR}	15°	26.3°	32.1°
No-load DC voltage at LCC, U_{di0NR}	229.3 kV	249.1 kV	265.5 kV
Converter transformer capacity, S_N	240.1 MVA	260.8 MVA	278.1MVA
Reactive power consumption, Q_d	215.1 Mvar	291.1 Mvar	344.5 Mvar
Conductive losses of thyristor, W1	566.3 W	568.7 W	569.5 W
Number of thyristors each bipole station	1440	1564	1668
Total losses of thyristor valves, in p.u. value	100%	108.6%	115.8%
Power losses of LCC converter transformer	618.2 kW	636.3 kW	645.2 kW
Reactive power consumption, in p.u. value	100%	135%	160%
FHMMC solution			
Resulting DC voltage in p.u. value at VSC side, η	1.0	0.91	0.84
Number FBSMs, M	0	1	2
Number HBSMs, N	23	22	21
Valve losses in p.u. value	100%	104%	109%

6. CONCLUSION

Hybrid HVDC has a special technical challenges i.e. the DC power discontinuation during AC voltage decrease at the LCC rectifier, which will result in the DC overvoltage and the disturbance at the receiving end AC system. To mitigate the DC power discontinuation of hybrid HVDC, the high firing angle operation of LCC is proposed and compared with the FHMMC solution. For U_{acmin}>90%·U_{lNR}, high firing angle solution has similar power losses compared with FHMMC solution, whereas the high firing angle solution has less modification on control and protection platform and could be the superior solution. However, for U_{acmin}<90%·U_{lNR}, the converter transformer cost as well as the cost AC filter cost for high firing angle solution will increase greatly, thus the FHMMC solution may be preferred.

References

[1] Zhao, Z., HVDC Application of GTO Voltage Source Inverters. 1992, PhD thesis, University of Toronto, Canada: Toronto, 1992.

[2] Zhao, Z. and M.R. Iravani, Application of GTO voltage source inverter in a hybrid HVDC link. *Power Delivery*, IEEE Transactions on, 1994. 9(1): p. 369-377.

[3] Iwatta, Y., et al. Simulation Study Of A Hybrid Hvdc System Composed Of A Self-commutated

Converter And A Line-commutated Converter. *AC and DC Power Transmission*, Sixth International Conference on (Conf. Publ. No. 423). 1996.
[4] Li, G., et al. Research on hybrid HVDC. *Power System Technology, PowerCon*, 2004.
[5] Torres-Olguin, R.E., M. Molinas, and T.M. Undeland. A controller in d-q synchronous reference frame for hybrid HVDC transmission system. *Power Electronics Conference (IPEC)*, 2010.
[6] Kotb, O. and V.K. Sood. A hybrid HVDC transmission system supplying a passive load. *Electric Power and Energy Conference (EPEC)*, 2010.
[7] Zhan, P., et al., Research on hybrid multi-terminal high voltage DC technology for offshore wind farm integration *Journal of Modern Power Systems and Clean Energy*, Vol 1(1), 2011: p32-39.
[8] Torres-Olguin, R.E., M. Molinas, and T. Undeland. Hybrid HVDC connection of large offshore wind farms to the AC grid. *Industrial Electronics (ISIE)*, 2012.
[9] Zhao C Y, Xu J Z, Li T. DC faults ride-through capability analysis of Full-Bridge MMC-MTDC System. *Sci China Tech Sci*, 2013, 56: p253-261.
[10] XU, F., XU Z., HVDC system Based on LCC and FHMMC. Vol.40 (8), *High Voltage Engineering*, 2014:p2520-2530.
[11] Hongbo, J. and A. Ekstrom, Multiterminal HVDC systems in urban areas of large cities. *Power Delivery*, IEEE Transactions on, 1998. 13(4): p. 1278-1284.
[12] US8737096. Tapping Power from a HVDC Transmission System, ABB, 2008.
[13] Nosaka, N., et al., Simulation Studies on A Control and Protection Scheme for Hybrid Multi-Terminal HVDC Systems. IEEE, 1998.
[14] WO2014111595A1. A multilevel converter with hybrid full-bridge cells. ABB, 2013.
[15] WO2011042050. Modified Voltage Source Converter Structure. ABB, 2011.
[16] Zhiyuan Zhao. HVDC application of GTO voltage source inverters. PhD thesis, University of Toronto, 1992: p80.
[17] HUANG Fang-neng, LIANG Xiao-bing, GU Nan-feng, et al. Harmonic Analysis in Parallel Operation of TSQ-GBJ HVDC/AC Transmission System. *Guangxi Electric Power*, 2002 (3)：p1-9.
[18] Zhao Wanjun. HVDC transmission engineering technology. *China Electric Power Press*, Beijing, 2008.